Automatic tuning strategies for model-based diagnosis methods applied to a rocket engine demonstrator

A. Iannetti[1], J. Marzat[2], H. Piet Lahanier[2] and G. Ordonneau[2]

[1]*Launcher directorate, CNES, Paris, France*
alessandra.iannetti@cnes.fr

[2]*ONERA-The French Aerospace Lab -Palaiseau, France*
julien.marzat@onera.fr
helene.piet-lahanier@onera.fr
gerard.ordonneau@onera.fr

ABSTRACT

Rocket engines are complex and critical systems mostly relying on simple redlines strategies for monitoring the main functional parameters. This approach is typical on expendable rockets with non-adjustable valves because in case of failure the only possible action is to cut off the engine. Anyway years of experiments on engine firings or subsystem benches show that there is space for an update of the monitoring strategies because this would lead to a reduction of false alarm rates and to an improved exploitation of test hardware. Moreover real-time diagnosis methods will be necessary in case of design of intelligent rocket engine controllers for next generation reusable launchers. The work presented in this paper is part of a demonstration project of new diagnosis tools for rocket engines applied to the cryogenic combustion bench Mascotte. This bench developed by ONERA and CNES is used to analyze combustion and nozzle expansion characteristics of cryogenic fuels such as oxygen and hydrogen or methane. Model-based diagnosis tools have been developed for the combustion chamber and nozzle water cooling circuit. The basis was the setup of simplified expressions for modeling the functional behavior of the water circuit and then the development of predictive strategies such as parameter identification and Kalman filters. Anomalous event detection is obtained via residual analysis based on a CUSUM test. This paper presents the new automatic tuning strategies for the CUSUM threshold setting and the detection results obtained on Mascotte firing data.

1. INTRODUCTION

During the last decades, several research efforts have been conducted to improve the diagnosis methods of rocket engines for applications at test bench or during flight (Benoit, Bonert, Legonidec, Supié, 2009), (Iannetti, 2014), (Wu, J., 2005). Current monitoring strategies rely mostly on redline systems which are set on critical parameters. This methodology is easy to put into place but it demands fine expertise to correctly tune the physical values of the thresholds and it requires sensors at critical locations which is not always possible. The process of selecting the feared events, defining the sensing locations, deciding the allowed thresholds for the engine functioning is critical for a successful monitoring (Cicanek, 1984). Errors in thresholds assignment may results in unjustified engine aborts with mission objectives loss for flight as well as for test bench campaigns. This risk is increased when the engine operates at various regimes and it is necessary to adapt the thresholds. For classical rockets this is especially the case for the test bench application but it is an important issue to consider for future engines with regulation systems.

The work presented here is the latest step of a development effort (Iannetti, Marzat, Piet-Lahanier et al., 2015) focused at demonstrating the potential of model-based diagnosis algorithms for liquid rocket engine monitoring.

A cryogenic test bench was selected as benchmark application of this research. The previous works (Iannetti, Marzat, Piet-Lahanier, Ordonneau, 2015) resulted in the development of model-based detection algorithms that have been validated for the cooling system of the Mascotte bench. Anomalous event detection is obtained via residual analysis based on a CUSUM test. After a brief review of the

bench and of the algorithms in sections 2 and 3, we describe in sections 4, 5 and 6 the new contribution consisting of two automatic strategies for the tuning of the detection threshold used in the CUSUM test. Detection results on Mascotte firing data are presented to support the analysis.

2. MASCOTTE TEST BENCH

The Mascotte test bench runs cryogenics oxygen, hydrogen and methane. Its main components are the combustion chamber with the injector part and cooling jacket and the bi-dimensional nozzle called ATAC-HRM (Ordonneau, Hervat, Vingert, Petitot, Pouffary, 2013).

Typical operational pressures in the combustion chamber are up to 60bar and mixture ratios up to 6 (combustion temperature up to 3500K).

The cooling system is a water circuit inside the chamber and nozzle walls. The fluid is water provided by the bench feeding system. The good functioning of the circuit is vital for the success of each test as it allows keeping safety margin on the combustion chamber walls. Pressures, temperatures at inlet and outlet of each section of the water circuit and mass flow are monitored all along the test and whenever a measurement is out of range the test is stopped.

3. MODEL-BASED DIAGNOSIS ALGORITHMS

The model-based diagnosis strategy (Iannetti, Marzat, Lahanier, 2014), (Ding, 2008), (Marzat et al., 2012) consists in identifying one characteristic parameter of the hydraulic behavior via parameter identification technics (Isermann,1984), then to provide a parallel pressure estimation based on signals and the prediction of nominal model characteristics via an extended Kalman filter (Chow and Willsky, 1984). For the thermal behavior one Kalman filter was developed as well but this aspect is not presented in this paper. The model details can be found in (Iannetti et al. 2014, Iannetti et al. 2015) together with validation on test bench firings. In the work presented here we focus on the hydraulic behavior to test the detection performance when different residual analysis approaches are used.

Starting from conservation laws we derived a simplified functional model that could be applied to each section of the water circuit where pressure, temperature and mass flow are available.

The expression of the pressure evolution with time in a cavity fed by one orifice is provided in Eq. (1).

$$\frac{dP_2}{dt} = \left(\sqrt{\frac{P_1 - P_2}{k_p} \cdot \rho S^2} - q_2^s \right) \cdot \frac{a^2}{V_2} \qquad (1)$$

P_1: pressure in cavity 1 (Pa)
P_2: pressure in cavity 2 (Pa)
k_p : pressure drop coefficient (non dimensional)
ρ : water density (kg/m^3)
a : speed of sound in water (m/s)
V_2 : volume of cavity 2 (m^3)
S : cross sectional area for the orifice element (m^2)
$q = q_1^s = q_2^e$: mass flow through the orifice element / outlet mass flow from cavity 1/ inlet mass flow to cavity 2 (kg/s)

A simplified expression for k_p,using Blasius correlation, allows to explicit the link with the mass flow which is directly measured at the outlet of the "cavity".

$$k_p = 0.3164 \cdot \left(\frac{q}{\frac{\pi D_h}{4} \cdot \mu} \right)^{-0.25} \cdot \frac{L}{D_h} \cdot \frac{1}{2} \qquad (2)$$

μ = dynamic viscosity (kg/(s m))
D_h= characteristic dimension cross flow, hydraulic diameter
L = characteristic length of the flow

Thanks to Eq. (2) the pressure evolution with time can be further simplified by introducing parameter *M* that only depends on the geometry of the setup and on the fluid viscosity.

$$M = 0.3164 \cdot \left(\frac{1}{\frac{\pi D_h}{4} \cdot \mu} \right)^{-0.25} \cdot \frac{L}{D_h} \cdot \frac{1}{2} \qquad (3)$$

The overall expression for the pressure evolution with time is given in Eq. (4).

$$\dot{P_2} = \frac{a^2}{V_2} \cdot \left(-q_2\,(t) + q_2^{0.125}(t) \cdot \sqrt{\frac{\rho \cdot S^2}{M}} \cdot \sqrt{P_1(t) - P_2(t)} \right) \qquad (4)$$

This expression for the hydraulic behavior of the water cooling circuit is used for parameter identification or Kalman filter to provide process observer for real time detection of faulty behaviors.

3.1. Parameter identification for hydraulic characteristic behavior

When considering equation (4) in steady state condition and introducing parameter, $M = \left(\frac{\rho \cdot S^2}{M}\right)^{\frac{1}{2}}$, we obtain a further simplified expression between pressure and mass-flow measurement as given in Eq. (5).

$$q_2(t) = c \cdot q_2^{0.125}(t) \cdot \sqrt{P_1(t) - P_2(t)} \qquad (5)$$

A recursive least-square identification algorithm is used for estimating the value of *c* based on the measurementsq_2 , P_1 and P_2 , respectively outlet mass flow, inlet and outlet pressure.

3.2. Kalman filter for pressure estimation

Considering the time derivative of the pressure as non-negligible we introduce parameter $b = \frac{a^2}{V}$ and parameter

$d = b \cdot c$. We consider that the evolution of the new parameter d with time is negligible in the observed process and the dynamic system used for the extended Kalman filter is given in Eqs (6).

$$\dot{P}_2 = -bq_2\ (t) + d \cdot q_2^{0.125}(t) \cdot \sqrt{P_1(t) - P_2(t)} \qquad (6)$$
$$\dot{d} = 0$$

The Kalman estimation provides the outlet pressure and the parameter d based on the input measurements of inlet pressure and mass-flow.

4. RESIDUAL ANALYSIS: CUSUM TEST

Thanks to the monitoring tools developed, we are able to provide a prediction of specific measurement or characteristic parameter of the water circuit. To obtain a diagnosis flag it is necessary to compare the prediction with the measurement or the identified parameter. This is performed with a CUSUM test approach, a very common test to detect changes in data, where no statistical hypothesis are necessary (Basseville, Nikiforov, 1993), (Marzat, Walter, Piet-Lahanier, Damongeot, 2010).

Equations (7) below give the expression of the CUSUM sums.

$$S_1(t) = \max\ (S_1(t-1) + r(t) - \delta, 0) \qquad (7)$$
$$S_2(t) = \max\ (S_2(t-1) - r(t) - \delta, 0)$$

The parameter δ is the minimal size of the faulty variation that can be detected. The decision rule is if $S_1 > \lambda \cdot \delta$ or $S_2 > \lambda \cdot \delta$ decide fault, else decide no fault. The parameter λ is a user threshold that allows reducing flag sensitivity to small non persistent changes. r(t) is the residual obtained thanks to the model-based algorithm: it is the difference between the identified parameter and its mean value estimated over time, or it is the Kalman filter residual obtained as the difference between the filter estimation and the acquired measure.

5. TEST DATA AND DETECTION OBJECTIVES

A number of tests from past Mascotte firing campaign were considered for validation of the detection strategies with the automatic tuning of δ. We focus on the following monitored variables: pressures, mass flow and temperature signals located at the inlet and outlet of a section of the water cooling system. The results presented here focus on a test from 2014 where some abnormal evolutions in the outlet pressure signal were gone undetected by conventional bench redlines. During post-test analysis these events turned out to be linked to leakages in the water circuit of the nozzle and could have potentially led to critical failure of the test. Figures below show the evolution of inlet, outlet pressure, and mass flow. It should be noted that these faults are of very limited amplitude and thus barely detectable. Therefore, the results presented and the associated tunings should be considered in this context.

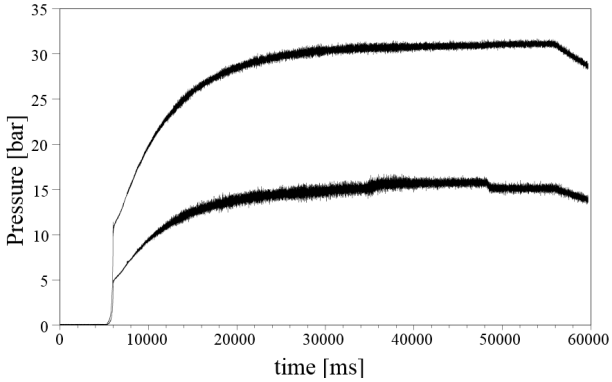

Figure 1. Pressure signals for the reference test

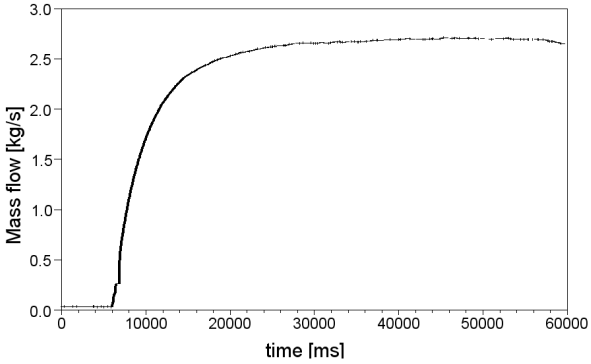

Figure 2. Mass flow signal for the reference test

These signals are directly used by the bench control system for redlines monitoring. As it can be seen from the pressure curves the signal noise is increasing from the beginning to the end of the test and in the outlet pressure signals we can identify the following main events:

- Event n°1 : 35s<t<40s start of transient of small pressure fluctuations mixed with some increased sensor noise
- Event n°2: 48s<t<49s end of pressure fluctuation and signal back t nominal value
- Event n°3: t=56s beginning of stop transient

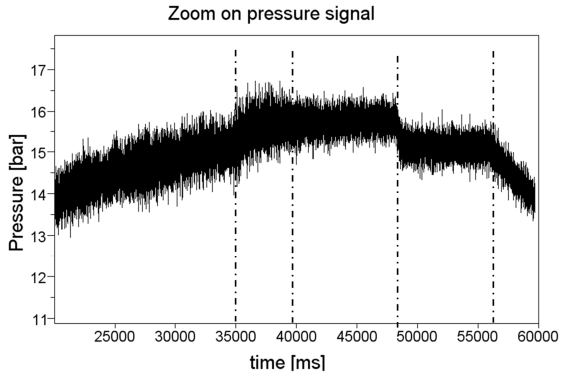

Figure 3. Pressure signal and main events

In the next sections we describe the tuning strategies and the results of event detection for the parameter identification algorithm and the Kalman estimator when coupled with the automatic tuning method for the CUSUM test. The detection analysis is tested over the ability to adapt to sensor noise evolutions and on the detection of the main events.

6. AUTOMATIC THRESHOLDS TUNING STRATEGIES

In order to correctly determine the δ for detection two methods have been tested:

- Standard deviation of estimation residual
- Maximum deviation of estimation residual

6.1. Standard deviation of estimated residual

Here the parameter δ is calculated with the following method as expressed in Eqs (8) and (9).

$$\delta(t) = t_{det} \cdot \sqrt{\frac{1}{N} \cdot \sum_{i=t-\theta}^{t} (r(i) - \hat{r})} \quad (8)$$

$$\delta(t) = \alpha \cdot \delta(t - dt) + (1 - \alpha) \cdot t_{det} \cdot \sqrt{\frac{1}{N} \cdot \sum_{i=t-\theta}^{t} (r(t) - \hat{r})} \quad (9)$$

Where *r(t)* is the residual and $\hat{r}$ is the allowed average reference value given by the difference between the estimated parameter *c* and its average over the latest time interval for the parameter identification method, or the Kalman estimation residual for the other algorithm.

The following parameters have to be tuned:

- t_{det}: for standard noise distribution this parameter allows to define a statistical threshold around the mean value of the parameter. For example for t_{det} =3 we cover 99.7% of probability of noise behavior.
- λ: this parameter is linked to the CUSUM sums and allows to tune the algorithm detection sensitivity
- α: this parameter allows to provide a first-order temporal filtering of δ during online calculation to reject random fluctuations
- θ: this parameter corresponds to a time window and depending on the calculation frequency it gives the number of samples used to estimate the reference δ. In the analysis shown here the acquisition rate is 1000Hz and the value of θ is given in number of samples. Its value has an impact on the mean calculation and a good compromise has to be selected to improve algorithms implementation for real time application. A bigger buffer of data will require larger memory allocations and thus overall calculation time.

6.2. Maximum variation of estimated residual

Another possible strategy is to identify the maximum variation of the residual over a nominal period of the test run.

$$\delta = t_{det} \cdot \max_{i=t-\theta:t} ||r(i)|| \quad (10)$$

$$\delta(t) = \alpha \cdot \delta(t - dt) + (1 - \alpha) \cdot t_{det} \cdot max_{i=t-\theta:t} ||r(i)|| \quad (11)$$

The definitions of the residual and parameters to be tuned are the same as for the standard deviation method with the difference that t_{det} in this case does not have an indication of probability of detection.

7. RESULTS FOR PARAMETER IDENTIFICATION

7.1. Adaptive threshold based on standard deviation

Figure 4 shows the results of the automatic calculation with $t_{det} = 3$, corresponding to a statistical probability of 95.5% of detection, α = 0.97 and θ= 500 pts.

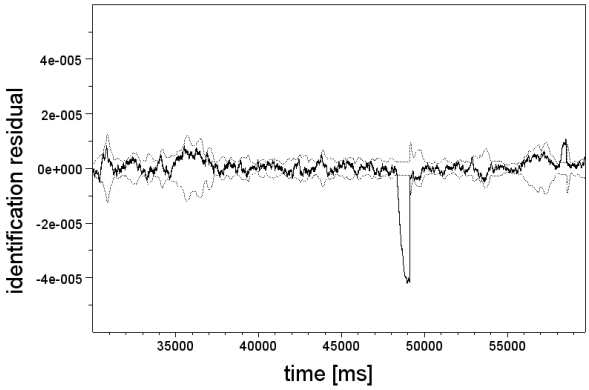

Figure 4. Evolution of threshold δ (dotted line) and detection residual (solid line) for standard deviation method

At main event n°1 the residual approaches the upper threshold but no important violations are seen. Event n°2 is clearly visible around 48s and the estimated residual violates the lower limit. In this case the automatic δ calculation filters enough the residual variation so that the induced increase of the threshold is limited and stays within the range of the allowed nominal variations.

Figure 5 shows the detection results with the indicated setting for the threshold calculation and λ=2.

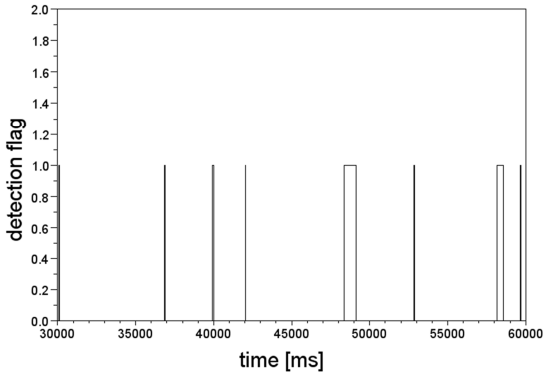

Figure 5. Detection flags for standard deviation threshold

To reduce sensitivity to small events it is necessary to increase the λ factor or the minimum size of the δ. This choice is a compromise for the detection accuracy.

With an increased size of δ, for example 4 times the standard deviation and the same λ we obtain detection of events n°1 and 2, corresponding to the main "abnormal" fluctuations between. Detection flags are shown in Figure 6.

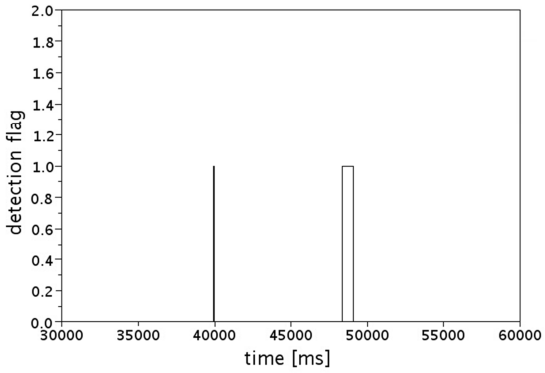

Figure 6. Detection flag for standard deviation δ

Increasing the size of θ allows filtering out parameter evolutions linked to noise levels but it also reduces detection sensitivity.

7.2. Adaptive threshold based on maximum variation

The maximum variation is by definition the largest residual allowed during the latest nominal operations so the size of δ should not be modified. The only tuned parameter is thus λ.

Results of the automatic calculation of δ with t_{det}=1 are shown in Figure 7 (other settings are λ=7, α = 0.97 and θ=500).

The adaptive threshold follows the residual variations and as for the standard deviation method it allows to detect clearly main event n°2 but the faulty variation has an important impact on the threshold itself and results in a temporary increase of the upper and lower limits just after the event.

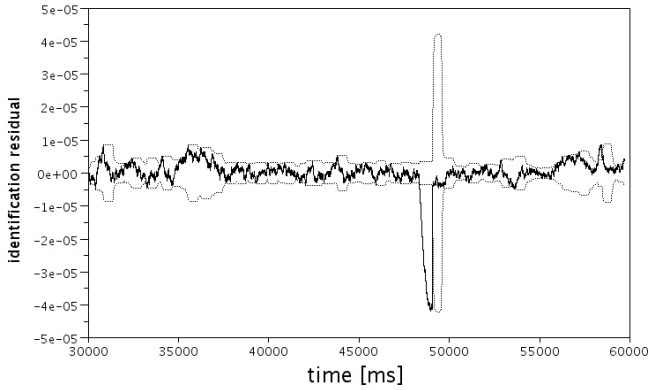

Figure 7. Evolution of threshold δ (dotted line) and detection residual (solid line) for maximum variation method

This behavior might be improved by introducing a delay on the threshold evaluation after the detection but it would in turn result in a loss of sensitivity.

The detection flag is provided in Figure 8 with a t_{det}=1 and λ=7, α = 0.97 and θ=500. These are the settings that provided the most accurate detection flags.

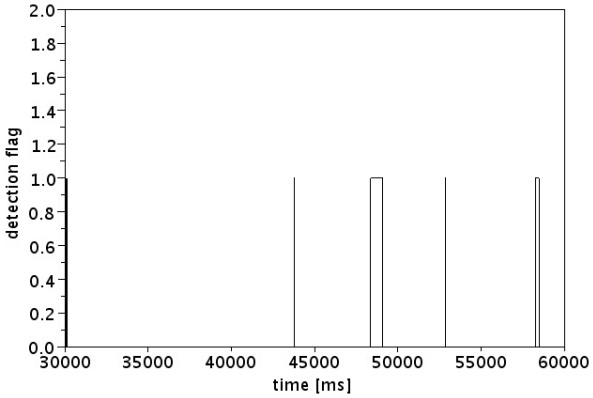

Figure 8. Detection flag with maximum variation δ

To reduce the number of false alarms, such as the flag between 50s and 55s, a very large λ up to 7 times the

minimum fault size is needed, which puts into question fault sensitivity

When calculating the maximum variation, the buffer length considered can have an impact on the detection sensitivity as there could be transient effects. With a smaller buffer of 10 points, a similar detection performance is obtained by setting a smaller λ = 4. This implies that a variation of lower intensity could also be detected. As shown in Figure 6, detection flags are raised in coherence with the events in Figure 3 and with no false alarm.

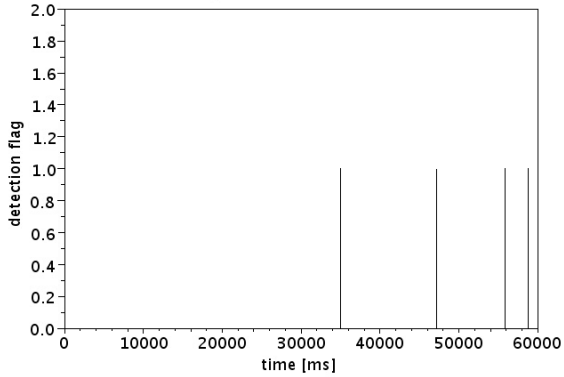

Figure 9. Detection flag with reduced buffer

8. RESULTS FOR PRESSURE KALMAN ESTIMATION

8.1. Adaptive threshold based on standard deviation

Figure 10 shows the results of the automatic calculation with $t_{det} = 3$, α = 0.97 and θ= 500 pts.

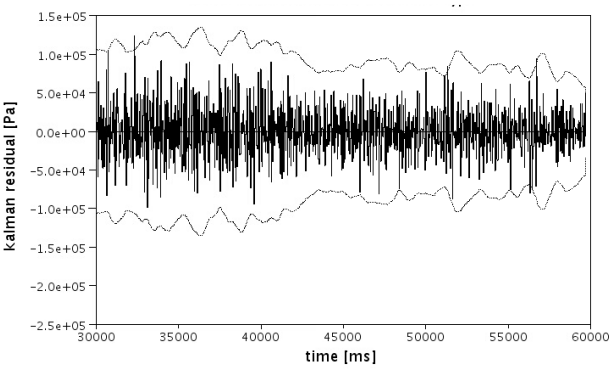

Figure 10. Evolution of threshold δ (dotted line) and detection residual (solid line) for standard deviation method

The behavior of the Kalman residual is different from the one of parameter identification. By definition the Kalman filter is able to adapt to transients and it takes into account the noise level. As a consequence the algorithm is less sensitive to the level of fluctuations of the reference test. The most important parameter to define the detection sensitivity is the ratio of the fluctuations to the average noise level.

With a t_{det}=3, λ=2, α = 0.97 and θ = 500 no detection is achieved.

With a smaller threshold t_{det}=1, see Figure 11, the results are not improved. Beside the detection of the stop transient, flags are raised at 30s and 50s in relations to noise increase and can be considered as false alarms.

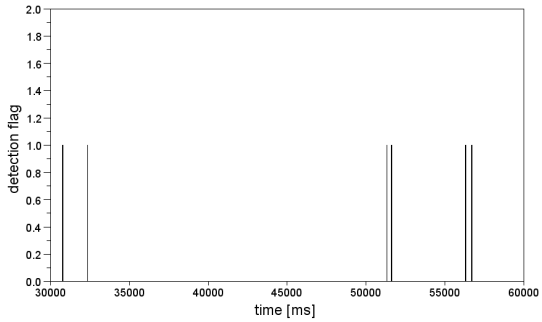

Figure 11. Detection flags with standard deviation δ

8.2. Adaptive threshold based on maximum variation

The results for the automatic calculation of δ based on the maximum variation with t_{det}=1, λ= 2, α = 0.97 and θ =500 are shown in Figure 12. With these settings no detection is achieved. To improve this, we reduced the buffer as θ=10. This has a direct impact on δ. The detection results are not much improved with t_{det}=1, λ=2 and θ =10 as shown in Figure 13.

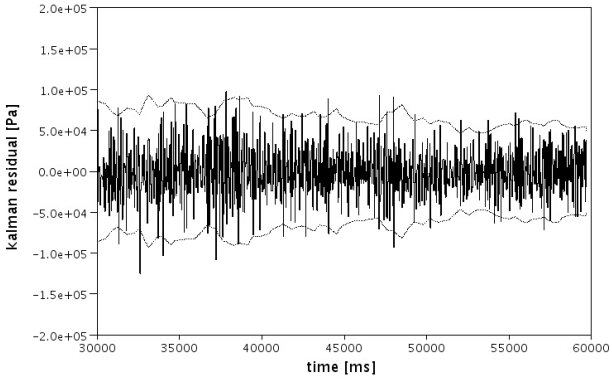

Figure 12. Evolution of threshold δ (dotted line) and detection residual (solid line) for maximum variation method

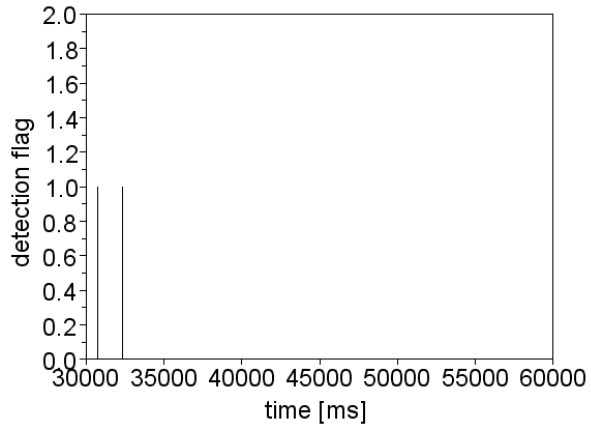

Figure 13. Detection flag with maximum variation δ

9. DISCUSSION

The results obtained show a good detection performance with the parameter identification approach and a standard deviation method for the tuning of the CUSUM threshold. Figure 6 shows that detection of the two main abnormal events is obtained. To improve this behavior, the maximum variation type helps by providing detection of the stop transient as well. Figure 9 shows that flags are raised as expected. The standard deviation method is still preferable as it is more robust to the sample size and in case of detection is less impacted by the residual variation. The downside is an increased calculation load with respect to the maximum approach.

Detection with the Kalman filter of these very small faults is more difficult as the level of fluctuations with respect to the sensor noise is too low. With both methods of threshold calculation the detection flags cannot isolate the events. With a standard deviation method and t_{det}=3 no detection is possible and with decreased t_{det} only the stop transient is detected. This result is nevertheless encouraging with respect to detection robustness and further analysis on larger faults shall be performed.

10. CONCLUSIONS

Adaptive tuning strategies are at the basis of any model-based diagnosis system. The algorithms developed in previous works (Iannetti, Marzat, Piet-Lahanier, Ordonneau 2015), allowed calculation of detection residuals that have to be analyzed via a decision logic. The CUSUM test was chosen but it requires setting of a detection threshold. To automatically choose its value two tuning strategies were developed and presented in this paper. The remaining parameters to set are mainly generic and do not depend on the test targets. For the standard deviation approach the settings also implicitly provide a statistical meaning to the detection threshold. The maximum variation method is supposed to be more reliable against false alarms but it proved to be more difficult to tune. The impact of the tuning methods also depends on the specific algorithm: the tuning settings are not the same for parameter identification and Kalman filters, which are based on different models of the system.

The objective of the new tools with respect to the classical redline monitoring is to detect small changes within shorter reaction time but also to provide generic tools that do not need a threshold setting dependent on the engine operating point. This has been obtained thanks to the proposed strategies.

The results over the test case have shown good overall potential to detect very small events. Although the main parameters have to be tested and thoroughly analyzed before going into application for run time operation, once they are set they are independent from the specific engine operating point.

REFERENCES

Benoit, S. P.Bonert, S. Legonidec, P. Supié, (2009), *A diagnostic demonstrator: a platform for the evaluation of real time diagnostic data dedicated to space engines*, Conference of the Society for Machinery Failure Prevention Technology (MFPT), Dayton OH, USA.

Blanke, M., Kinnaert, M., Lunze, J., Staroswiecki, M., (2003). *Diagnosis and Fault-Tolerant Control*. Springer Verlag, Berlin Heidelberg.

Chow, E., Willsky, A.S., (1984), *Analytical redundancy and the design of robust failure detection systems,* IEEE Transactions on Automatic Control, Vol. 29(7), pages 603-614.

Cicanek, H., (1985), *Space Shuttle main engine failure detection,* American Control Conference, Boston MA, USA.

Ding, S.X., (2008), *Model-based fault diagnosis techniques*, Springer Verlag, Berlin Heidelberg.

Iannetti, A., (2014). *Overview on European efforts on health monitoring/management systems for rocket engines.* Space Propulsion Conference, Köln, Germany.

Iannetti, A., Marzat, J., Piet-Lahanier, H. et al., (2014), *Development of model based fault diagnosis algorithms for the Mascotte cryogenic test bench.* IOP Journal of Physics: Conference Series, Vol 570, number 7.

Iannetti, A., Marzat, J., Piet-Lahanier, H. et al., (2015), *Fault diagnosis benchmark for a rocket engine demonstrator*. 9th IFAC Symposium on Fault Detection Supervision and Safety for Technical Processes, Paris, France, IFAC-PapersOnLine 48(21), pages 895-900.

Iannetti, A., Marzat, J., Piet-Lahanier, H., Ordonneau, G. et al., (2015), *HMS developments for the rocket engine demonstrator Mascotte*. 51st AIAA/SAE/ASEE joint Propulsion Conference.

Isermann, R., (1984). *Process fault detection based on modeling and estimation methods—a survey*. Automatica, Vol. 20(4), pages 387-404.

Marzat, J., Walter, E., Piet-Lahanier, H., Damongeot, F., (2010), *Automatic tuning via kriging-based optimization of methods for fault detection and isolation*, IEEE Conference on Control and Fault-Tolerant systems, Nice, France, pages 505-510.

Marzat, J., Piet-Lahanier, H., Damongeot, F., Walter, E., (2012), *Model based fault diagnosis for aerospace systems: a survey*, Proceedings of the Institution of Mechanical Engineers, Part G: Journal of aerospace engineering, Vol. 226(10), pages 1329-1360.

M. Basseville and I. V. Nikiforov. *Detection of Abrupt Changes: Theory and Application.* Prentice Hall Englewood Cliffs, NJ, 1993.

Ordonneau, G., Hervat, P., Vingert, L., Petitot, S., Pouffary, B., (2013), *First results of heat transfer measurements in a new water-cooled combustor on the Mascotte facility*, 4th European conference for aerospace sciences (EUCASS), Munich, Germany.

Wu, J., (2005), *Liquid propellant rocket engines health monitoring- a survey*, ACTA Astronautica, Vol. 56, pages 347-356.